# Amyloid Nucleation Triggered by Agitation of $\beta_2$-Microglobulin under Acidic and Neutral pH Conditions

Kenji Sasahara,[‡] Hisashi Yagi,[‡] Miyo Sakai,[‡] Hironobu Naiki,[§] and Yuji Goto*,[‡]

*Institute for Protein Research, Osaka University and CREST, Japan Science and Technology Agency, Yamadaoka 3-2, Suita, Osaka 565-0871, Japan, and Faculty of Medical Sciences, University of Fukui and CREST, Japan Science and Technology Agency, Eiheiji, Fukui 910-1193, Japan*

*Received October 1, 2007; Revised Manuscript Received November 28, 2007*

ABSTRACT: Amyloid nucleation through agitation was studied with $\beta_2$-microglobulin, which is responsible for dialysis-related amyloidosis, in the presence of salt under acid and neutral pH conditions. First, the aggregation of $\beta_2$-microglobulin in NaCl solutions was achieved by mildly agitating for 24 h at 37 °C protein solutions in three different states: acid-unfolded, salt-induced protofibrillar, and native. The formation of aggregates was confirmed by an increase in light scattering intensity of the solutions. Then, the aggregated samples were incubated without agitation at 37 °C for up to 25−45 days. The structural changes in the aggregated state during the incubation period were examined by means of fluorescence spectroscopy with thioflavin T, circular dichroism spectroscopy, and electron microscopy. The results revealed that all the samples in the different states produced a mature amyloid nucleus upon agitation, after which the fibrils elongated without any detectable lag phase during the incubation, with the acid-unfolded protein better suited to undergoing the structural rearrangements necessary to form amyloid fibrils than the more structured forms. The amount of aggregate including the amyloid nucleus produced by agitation from the native conformation at neutral pH was estimated to be about 9% of all the protein by an analysis using ultracentrifugation. Additionally, amyloid nucleation by agitation was similarly achieved for a different protein, hen egg-white lysozyme, in 0.5 M NaCl solution at neutral pH. Taken together, the agitation-treated aggregates of both proteins have a high propensity to produce an amyloid nucleus even at neutral pH, providing evidence that the aggregation pathway involves amyloid nucleation under entirely native conditions.

$\beta_2$-Microglobulin ($\beta$2-m[1]), a typical immunoglobulin domain consisting of 99 residues, constitutes the noncovalently bound light chain of the major histocompatibility complex type I (*1*). In its native form, this protein has a $\beta$-sandwich fold involving seven $\beta$-strands stabilized by a single disulfide bond (*2*, *3*). Dialysis-related amyloidosis (DRA), a disease arising as a serious complication in patients on long-term hemodialysis, involves the deposition of amyloid fibrils consisting primarily of $\beta$2-m in bones and ligaments (*4*−*6*). Amyloid fibrils are recognized as a pathological hallmark of a variety of amyloid diseases, such as Alzheimer's disease, Parkinson's disease, the transmissible spongiform encephalopathies, and type II diabetes (*7*, *8*). The main chain backbone of amyloid fibrils has a common structural motif consisting of cross $\beta$-sheets in which the strands are arranged perpendicular to the fibril axis (*9*). However, the mechanism by which amyloid fibrils are formed remains unclear.

In healthy individuals, $\beta$2-m is released from the major histocompatibility complex type I and transported in plasma to the kidneys where the majority of the protein is excreted by degradation (*4*−*6*). However, in patients undergoing hemodialysis, $\beta$2-m is not efficiently cleared from the serum by the kidneys or the dialysis membrane, and so the circulating concentration of the protein increases up to 60-fold, resulting in the deposition of amyloid fibrils predominantly in the joint spaces (*4*−*6*). Although the rise in the concentration of $\beta$2-m seems necessary, it in itself does not cause the onset of DRA; complex factors such as the type of dialysis membrane used, the duration of dialysis treatment, and the age of the patient may be involved (*4*, *5*, *10*, *11*). How $\beta$2-m assembles to form amyloid fibrils in vivo is not currently well understood.

In vitro, under acidic conditions at pH 2.5 where $\beta$2-m is acid-unfolded, fibrillar structures are formed by at least two parallel routes, depending on the ionic strength of the solution (*6*, *12*, *13*). In the presence of ∼0.2 M NaCl (i.e., low ionic strength), well-organized mature fibrils with a long (∼$\mu$m) and needle-like morphology (10−20 nm in diameter), typical of amyloid fibrils accumulated in osteoarticular tissues, are formed via a nucleation−polymerization mechanism involving the formation of a nucleus in a lag phase, after which the fibrils elongate rapidly. Addition of preformed seed fibrils (i.e., fragmented fibrils) to the monomeric precursors ef-

* Author to whom correspondence should be addressed. Phone: +81-6-6879-8614; fax: +81-6-6879-8616; ygoto@protein.osaka-u.ac.jp.

‡ IPR, Osaka University.

§ University of Fukui.

[1] Abbreviations: $\beta$2-m, $\beta_2$-microglobulin; DRA, dialysis-related amyloidosis; ITC, isothermal titration calorimeter; CD, circular dichroism; EM, electron microscopy; SDS, sodium dodecyl sulfate; ThT, thioflavin T; HEWL, hen egg-white lysozyme; WL, worm-like.

10.1021/bi701968g CCC: $40.75 
Published on Web 01/23/2008

fectively bypasses the nucleation step, leading to a rapid elongation without the lag phase (*14*). In contrast, at high concentrations of salt (~0.5 M NaCl), $\beta$2-m is able to rapidly form worm-like fibrils (WL fibrils) with distinct morphological features without a lag phase: short, curved, and thin fibrils (<600 nm in length, 2−5 nm in diameter). In some cases, thin fibrils like this have been purported to be direct precursors of mature amyloid fibrils (*15*), whereas in other cases, the role of an off-pathway has been proposed (*16*−*19*). In the case of $\beta$2-m, the WL fibrils and mature fibrils have been shown to form via distinct and competitive pathways (*6*, *12*, *13*). The molecular mechanisms leading to the distinct pathways and morphological features of fibrillation are not fully understood.

At neutral pH under physiologically relevant conditions in vitro where the protein is stably folded, amyloid fibrils of this protein have been formed following the addition of fibrillation-nucleating seed fibrils (*20*, *21*), the addition of trifluoroethanol or sodium dodecyl sulfate (SDS) (*22*, *23*), the addition of copper ions and urea (*24*), ultrasonication in the presence of SDS (*25*), a deletion of N-terminal residues (*26*), a mutation of terminal $\beta$-strands (*27*), and an agitation−heat treatment (*28*). That is, the formation of amyloid fibrils was found to require significant destabilization of the native protein, raising important questions about the identity of factors irritating the fibril nucleation in vivo.

In a previous study (*29*), we have shown that salt-induced WL fibrils of $\beta$2-m at pH 2.5 that were aggregated intentionally by agitation can be effectively converted into well-organized mature amyloid fibrils by heating them in the cell of a differential scanning calorimeter (DSC). Furthermore, $\beta$2-m aggregated intentionally by agitation under neutral pH conditions including high concentrations of NaCl was found to be efficiently converted into well-organized mature amyloid fibrils upon heating by DSC (*28*). In these studies, a notable point was that the conversion into mature amyloid fibrils was effectively triggered upon heating when the protein molecules were in the moderately aggregated state, which was considered as a scaffold to trigger the fibrillation, leading to the conformational rearrangement into a cross-$\beta$ structure via specific intermolecular interactions between adjacent molecules (*28*, *29*). In this study, we focus on the ability of agitation-treated aggregates of $\beta$2-m to induce fibril nucleation under acidic and neutral pH conditions. The results reveal that agitation-treated aggregation can promote dramatically the ability to form amyloid fibrils, resulting in amyloid nucleation. Amyloid nucleation was also achieved by agitation for a different globular protein, hen egg-white lysozyme (HEWL), at neutral pH.

## MATERIALS AND METHODS

*Materials.* Recombinant human $\beta$2-m was expressed in *Escherichia coli* and purified according to a procedure reported previously (*30*). Hen egg-white lysozyme (crystallized six times) was purchased from Seikagaku Co. Ltd. (Tokyo, Japan) and used without further purification. Citric acid monohydrate, NaCl, and SDS of analytical grade were obtained from Nacalai Tesque Inc. (Kyoto, Japan). Thioflavin T (ThT) was purchased from Wako Pure Chemical Industries Ltd. (Osaka, Japan). The stock solutions of NaCl (2 M), ThT (100 $\mu$M), and SDS (10 mM) were made in Milli-Q water and passed through a 0.22 $\mu$m pore-size filter. The citrate buffer at 250 mM was adjusted to pH 2.5 with NaOH (0.5 M) and used after the filtration (0.22 $\mu$m pore-size). The proteins were dissolved in Milli-Q water and passed through the same filter. The solution of $\beta$2-m in the acid-unfolded state was made in 50 mM citrate buffer at pH 2.5. Salt-induced WL fibrils of $\beta$2 m were spontaneously formed in 50 mM citrate buffer containing 0.5 M NaCl at pH 2.5. Solutions of $\beta$2-m and HEWL in the native state were prepared in 1.0 and 0.5 M NaCl solutions without buffer, respectively, in which the pH of the protein solution was 7.0−7.6. The concentrations of $\beta$2-m and HEWL were determined based on optical density at 280 nm using an extinction coefficient of 1.63 mL $mg^{-1}$ $cm^{-1}$ and 2.65 mL $mg^{-1}$ $cm^{-1}$, respectively (*30*, *31*).

*Agitation-Induced Aggregation of Proteins.* Agitation of the protein solutions was carried out at protein concentrations in the 30−60 $\mu$M range in the cell of an isothermal titration calorimeter (ITC) by stirring with the attached cylinder for 24 h at 310 rpm and 37 °C (VP-ITC, MicroCal, Northampton, MA) as described previously (*28*, *29*).

*Light Scattering Measurements and ThT Binding Assay.* Light scattering measurements and the ThT binding assay were performed with a Hitachi F-4500 spectrofluorometer using a quartz cell with a 5 mm path length. The wavelengths for excitation and emission were both set at 350 nm (2.5 nm slit width) in the light scattering measurements. For the ThT binding assay, aliquots of protein solution at 30 or 60 $\mu$M were mixed with Milli-Q water and 100 $\mu$M ThT, resulting in a solution containing 6 $\mu$M protein and 10 $\mu$M ThT. The intensity of the fluorescence from ThT in the mixed solution was measured with excitation at 445 nm (5 nm slit width) and emission at 485 nm (10 nm slit width). The temperature of the sample solutions was maintained at 25 ± 0.1 °C by circulating water from a thermostat.

*Seeding Reactions.* Acid-unfolded $\beta$2-m at 30 $\mu$M in 50 mM citrate buffer (pH 2.5) was incubated at 37 °C with seeds. The ThT binding assay was conducted for aliquots of the sample withdrawn at intervals. The seed fibrils were fragmented by sonication before mixing with the precursors.

*Sonication Treatment.* Sonication of the protein (aggregate) solution (50−400 $\mu$L) was carried out using a Microson sonicater (Misonix, Farmingdale, NY) at an intensity level of 2 with 20 times of a 1 s pulse on ice.

*Circular Dichroism.* CD measurements were carried out in a Jasco J-720 spectropolarimeter, using a quartz cell with a light length of 1 mm. The temperature of solutions was controlled by an electrically controlled cell holder attached to the polarimeter. Far-UC CD spectra were recorded at 25 °C. After the background from the buffer or solvent was subtracted, the data were converted into the mean residue ellipticity.

*Ultracentrifugation Measurements.* Sedimentation velocity data were obtained using a Beckman-Coulter Optima XL-I analytical ultracentrifuge with an An-60 rotor and two channel, charcoal-filled Epon cell for two samples of 48 $\mu$M $\beta$2-m solution containing 1.0 M NaCl at neutral pH: one is agitation-treated and the other is agitation-free. The absorbance data at 280 nm were collected at 10-min intervals by centrifugation at 181000*g* (52000 rpm) after incubation for 5 min at 27000*g* (20000 rpm) at 37 °C. The experimental sedimentation coefficients were obtained by analyzing the

Table 1: Structural State of the Protein and Solution Conditions Used

| state of protein | buffer | NaCl (M) | pH | protein concn ($\mu$M) |
|---|---|---|---|---|
| (1) acid-unfolded $\beta$2-m | citrate, 50 mM | 0 | 2.5 | 30 |
| (2) WL fibrillar $\beta$2-m | citrate, 50 mM | 0.5 | 2.5 | 30 |
| (3) native $\beta$2-m | − (water)[a] | 1.0 | 7.0−7.6 | 30, 60 |
| (4) native Lyz | − (water) | 0.5 | 7.0−7.6 | 30, 60 |

[a] Milli-Q water was used.

sedimentation velocity data and corrected to $S_{20,w}$ (standard solvent conditions: the density and velocity of pure water at 20 °C) using the software UltraScan 8.0.

*Electron Microscopy.* Transmission electron microscopy was used to visualize the aggregates and/or fibrils. The sample solution containing 30 or 60 $\mu$M protein was diluted 10-fold with Milli-Q water. An aliquot (5 $\mu$L) of the diluted solution was placed on a copper grid (400-mesh) covered by a carbon-coated collodion film for 60 s. After excess sample was removed by blotting with filter paper, 2% (w/v) uranyl acetate solution was then applied to the grids for a further 60 s. After the excess negative staining solution was removed with filter paper, the grids were air-dried. Electron micrographs were taken using a JEOL 100CX transmission microscope with a voltage accelerator of 80 kV. A magnification of 29000 was used.

## RESULTS

To investigate the effects of agitation-induced aggregation on the fibrillation, $\beta$2-m in three different conformational states was prepared at 30 $\mu$M: acid-unfolded $\beta$2-m at pH 2.5, WL fibrillar $\beta$2-m in the presence of 0.5 M NaCl at pH 2.5, and the native $\beta$2-m in the presence of 1.0 M NaCl at neutral pH (7.0−7.6). The details of the structural states of the protein and the solution conditions used are summarized in Table 1. For these samples, mild agitation was performed in the cell of the ITC instrument at 37 °C for 24 h by stirring with the attached cylinder that was inserted from the top exterior of the instrument into the cell through the narrow stem. The calorimeter's cell was used to ensure a stably controlled agitation and keep the solution/air interface to a minimum (*28*, *29*). An increase in the light scattering intensity of the agitation-treated samples was confirmed in comparison with that of the same samples before agitation, resulting in agitation-induced aggregation (Figure 1). Here, the high concentration of NaCl is necessary to produce the aggregation of some size by agitation under the neutral pH conditions. To clarify the effect of NaCl, agitation of the $\beta$2-m solution without NaCl at neutral pH was performed, showing only a little detectable aggregation (see sample 5 in Figure 1). Then, the aggregated samples were incubated without agitation at 37 °C for up to 25−45 days along with the same samples without the agitation treatment (i.e., control samples). The conformational changes in the aggregates during the incubation period were examined by means of a thioflavin T (ThT) binding assay, circular dichroism (CD) spectroscopy, and electron microscopy (EM).

*Conversion of $\beta$2-m in the Acid-Unfolded State into Mature Amyloid Fibrils at pH 2.5.* For the acid-unfolded $\beta$2-m, a direct comparison of fibrillation between the aggregated and control samples was obtained by measuring at time intervals the increase in the fluorescence of ThT, which emits fluorescence upon binding to amyloid fibrils (*32*): ThT binding assay. The fluorescence from the agitation-treated $\beta$2-m rapidly increased upon incubation without displaying a detectable lag phase and reached a markedly high value, about 2200 in Figure 2a in which the initial increase in ThT was enlarged in the inset. The data indicate that the aggregated sample formed specific aggregates with a high degree of ability to bind ThT. In contrast, enhanced fluorescence was not observed for the control sample during incubation for 25 days. The specific aggregates were found to be mature amyloid fibrils as shown below.

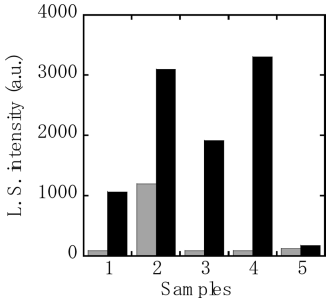


FIGURE 1: Agitation-induced aggregation of $\beta$2-m and HEWL. The light scattering intensity of $\beta$2-m and HEWL solutions (30 $\mu$M) was measured before (gray) and after (black) the agitation treatment. 1: $\beta$2-m in the acid-unfolded state at pH 2.5. 2: WL fibrils of $\beta$2-m in the presence of 0.5 M NaCl at pH 2.5. 3: $\beta$2-m in the native state in the presence of 1.0 M NaCl at pH 7.0−7.6. 4: HEWL in the native state in the presence of 0.5 M NaCl at pH 7.0−7.6. 5: $\beta$2-m in the native state in MQ water (without NaCl) at pH 7.0−7.6.

To examine the role as an amyloid nucleus of the specific aggregates formed from the agitation-treated aggregates, a seed-dependent extension reaction was carried out at pH 2.5, in which the specific aggregates were used as seeds; acid unfolded $\beta$2-m at 30 $\mu$M was incubated at 37 °C without agitation with the specific aggregates (final concentration, 0.67 $\mu$M) that were taken out after being incubated for 20 days. Aliquots of the sample were withdrawn at different time-points, and the ThT binding assay was carried out at 25 °C (Figure 2b). The fluorescence increased gradually without a lag phase, reaching a markedly high value of about 2100, a similar value to that obtained for the agitation-treated aggregates in Figure 2a. No increase in fluorescence was observed for the precursor solution without the addition of the specific aggregates. Therefore, the specific aggregates formed by the agitation−incubation method in Figure 2a acted as efficient seeds for the subsequent elongation after mixing with the precursors.

The high propensity of the agitation-treated aggregates to convert into a $\beta$-sheet structure was indicated by CD spectroscopy (Figure 2c). The CD spectrum of acid-unfolded $\beta$2-m (30 $\mu$M) at pH 2.5 was characterized by a broad negative band over the wavelength range of 200−250 nm, indicative of a substantial amount of unfolded structure (*12*, *33*). However, the sample subjected to agitation for 24 h (i.e., the agitation-treated aggregates) showed a CD spectrum with a somewhat intense signal at around 210−240 nm, implying the occurrence of some conformational change through the agitation treatment. The CD signal at 218 nm of the sample, typical of a $\beta$-sheet structure, became

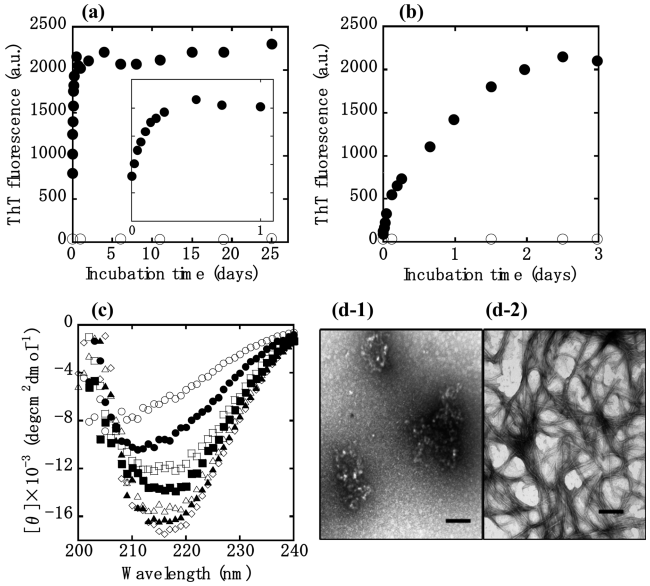


FIGURE 2: Conversion of $\beta$2-m in the acid-unfolded state into mature amyloid fibrils at pH 2.5. (a) Time course of fibril elongation of the agitation-treated, acid-unfolded $\beta$2-m (30 $\mu$M) at pH 2.5. Agitation-treated and control samples were incubated without agitation at 37 °C. The fibril elongation was assessed at various points during the incubation by the ThT binding assay. The initial increase in ThT fluorescence of the agitation-treated sample was enlarged in the inset. (●): agitation-treated sample, and (○): agitation-free sample. (b) Seeding reaction of acid-unfolded $\beta$2-m (30 $\mu$M) at pH 2.5. The acid-unfolded $\beta$2-m (30 $\mu$M) was incubated with and without seeds at 37 °C, in which the agitation-treated aggregates in panel a after incubation for 20 days were used as seeds (final concentration, 0.67 $\mu$M). The seeds were fragmented by the sonication treatment before use. The reactions were monitored by ThT binding assay at intervals. (●): with seeds and (○): without seeds. (c) Changes in the far-UV CD spectrum of the agitation-treated, acid-unfolded $\beta$2-m (30 $\mu$M) at pH 2.5. The CD spectra were recorded before (○) and after (●) agitation and at several stages of the incubation at 37 °C; (□): 1 h, (■): 2 h, (△): 5h: (▲): 72 h, and (◇): $\beta$2-m fibrils extended by the seeding reaction in panel b. (d) EM images of the acid-unfolded $\beta$2-m (30 $\mu$M) with and without the agitation treatment after being incubated for 20 days. (d-1): agitation-free sample; (d-2): agitation-treated sample. The scale bars represent 200 nm. Agitation was performed with the protein at 30 $\mu$M in the cell of an ITC for 24 h at 37 °C.

progressively more intense upon incubation without agitation at 37 °C (Figure 2c). The changes in the signal at 218 nm followed a similar trend to the evolution of the fluorescence of ThT (Figure 2a), a result suggesting that both features have a common origin. The CD spectrum of the agitation-treated aggregates after incubation for 3 days exhibited a high content of $\beta$-sheet structure, which was similar to that of the fibrils formed in the seeding experiments at pH 2.5 (Figure 2c), consistent with the similar saturated fluorescence of the two samples (Figure 2b).

To characterize the morphology of the specific aggregates, EM images of the agitation-treated and control samples were taken after incubation for 20 days (Figure 2d-1,2). The image of the control sample showed the morphology of amorphous-like aggregates without any ordered structure (Figure 2d-1), whereas the agitation-treated sample exhibited the presence of large quantities of mature amyloid fibrils with a well-defined morphology (fibril diameter 10−20 nm) (Figure 2d-2). Amorphous-like aggregates were rarely observed in the agitation-treated sample, indicating efficient conversion into amyloid fibrils. This observation is well consistent with the

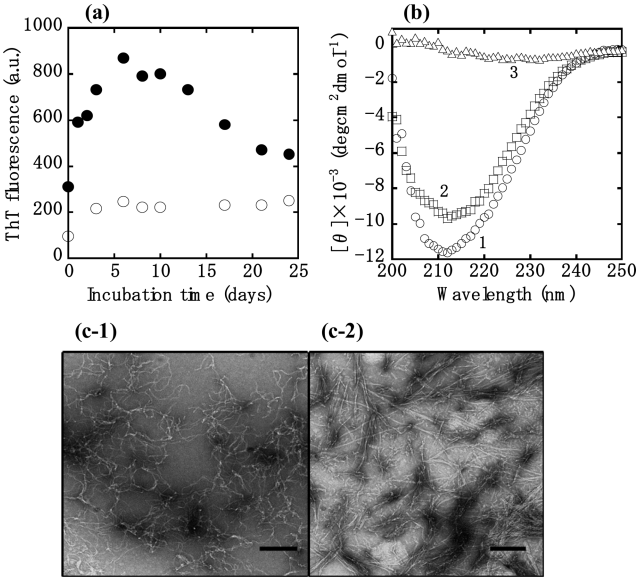


FIGURE 3: Conversion of $\beta$2-m in the WL fibrillar state into mature amyloid fibrils at pH 2.5. (a) Time course of the binding of ThT to the agitation-treated WL fibrils. The agitation-treated and control samples (30 $\mu$M WL fibrils) were incubated without agitation at 37 °C. The ThT binding assay was conducted at various points in time. (●): agitation-treated sample, and (○): agitation-free sample. (b) Far-UV CD spectra of the WL fibrils subjected to the agitation and incubation. 1: WL fibrils before agitation, 2: after agitation, 3: after agitation and incubation for 24 days. (c) EM images of the agitation-free (c-1) and agitation-treated (c-2) WL fibrils after the incubation. The images were taken after 24 days of incubation. The scale bars represent 200 nm. Agitation was performed as in Figure 1 with WL fibrils (30 $\mu$M) in the presence of 0.5 M NaCl at pH 2.5.

high content of $\beta$-sheet structure detected by CD spectroscopy (Figure 2c).

*Conversion of $\beta$2-m in the WL Fibrillar State into Mature Amyloid Fibrils at pH 2.5.* The salt-induced WL fibrils (30 $\mu$M) that formed in the presence of 0.5 M NaCl at pH 2.5 were similarly aggregated by agitation and incubated at 37 °C without agitation. Aggregation was confirmed by the enhanced light scattering intensity (Figure 1). Figure 3a shows the results of a ThT binding assay as a function of the incubation time for the agitation-treated and control samples. The fluorescence intensity was enhanced without a definite lag phase for the aggregated sample, reaching a maximum value of 870 after incubation for 6 days, and followed by a decrease. In contrast, the control sample showed a slight increase in ThT fluorescence immediately after the start of incubation and then reached a steady level of about 220.

Far-UV CD spectra of the WL fibrils were recorded to detect the conformational change accompanying the agitation and incubation (Figure 3b). The spectrum of the WL fibrils before agitation was characterized by a $\beta$-sheet spectrum with a minimum at around 212 nm, consistent with previous reports (*12*, *29*). Agitation of the fibril solution somewhat decreased the entire CD intensity but did not significantly affect the shape of the spectrum with the minimum peak. The agitation-treated aggregates taken out after 24 days of incubation exhibited an unusual CD spectrum with quite low intensities. Along with the result that ThT fluorescence reached a maximum during prolonged incubation (Figure 3a), the unusual CD spectrum suggests that a conformational

rearrangement of the aggregated WL fibrils into mature amyloid fibrils and further attendant aggregation took place upon incubation.

EM images of the aggregated and control fibrils taken out after 24 days of incubation were examined. The control sample exhibited a large number of WL fibrils with a thin, short, and curly appearance (Figure 3c-1). However, in the EM image of the agitation-treated sample, a quite different morphology was observed: mature amyloid fibrils and WL fibrils appeared to be mixed (Figure 3c-2). Consequently, together with the results of ThT fluorescence and CD spectra, the EM images indicate that the WL fibrils in the aggregated state were partly converted into mature amyloid fibrils, which could cause aggregation in the presence of 0.5 M NaCl as discussed below.

*Conversion of β2-m in the Native State into Mature Amyloid Fibrils at Neutral pH.* The fibrillation of β2-m under neutral pH conditions is one of the most important issues for understanding the pathology of DRA (*20*−*28*, *34*, *35*). It would be intriguing to know whether the agitation−incubation method initiates the fibrillation of β2-m in the presence of NaCl at neutral pH. Agitation of 30 μM β2-m in 1.0 M NaCl solution caused the formation of aggregates as indicated by an increase in light scattering intensity (Figure 1), consistent with a result reported previously (*28*). The time course of fibrillation during the incubation was likewise monitored by the ThT binding assay. Importantly, the intensity of the fluorescence from the agitation-treated sample was enhanced without a detectable lag phase, followed by a decrease, and reached a relatively constant value upon incubation extending to 48 days (filled circles in Figure 4a).

We repeated the same experiment with β2-m at a 2-fold higher concentration (i.e., 60 μM), finding very similar behavior to that at 30 μM (filled squares in Figure 4a). In contrast, the control samples without the agitation treatment did not show enhanced fluorescence over the same incubation period. It should be noted that no lag phase was observed in the plots of the ThT binding assay for the aggregated samples, suggesting that the amyloid nucleus is produced during the process of the agitation-induced aggregation. Furthermore, the decrease after the initial increase in fluorescence in Figure 4a suggests the aggregation of elongated fibrils.

The structural change responsible for the enhanced ThT fluorescence upon incubation as shown in Figure 4a was investigated by using far-UV CD spectra obtained at different points in the incubation (Figure 4b). The spectrum of 30 μM β2-m in 1.0 M NaCl solution before agitation (i.e., native β2-m) showed a weak minimum peak at around 220 nm, reflecting some contribution from the predominant β-structure. The spectral characteristic of the native secondary structure was apparently unaltered upon agitation (Figure 4b), confirming the persistence of the native-like secondary structure in the aggregated state. The changes in the spectrum for the agitation-treated sample were examined at different stages of the incubation (Figure 4b), showing that the CD spectrum after incubation for 40 days was superimposable on that before the agitation or incubation within the range of experimental uncertainty. The changes in ellipticity at 220 nm corresponding to the evolution of the β-sheet structure of the aggregated sample were plotted against incubation time in the inset in Figure 4b, confirming nondetectable variation

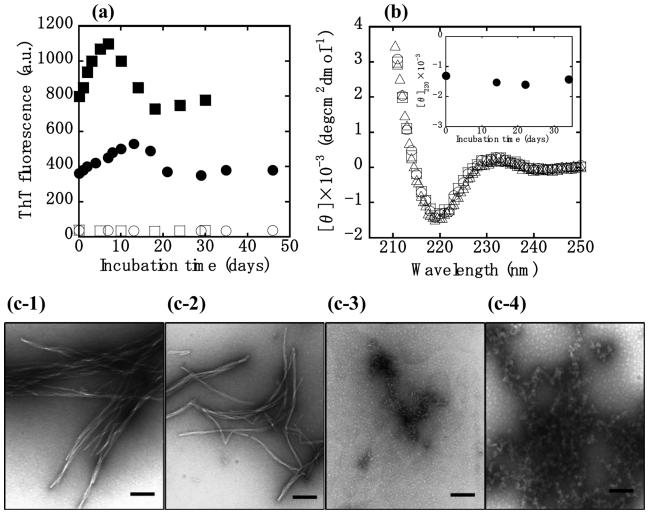


FIGURE 4: Conversion of β2-m in the native state into mature amyloid fibrils at neutral pH. Agitation was carried out as in Figure 1 with β2-m (30 and 60 μM) in 1.0 M NaCl solution at neutral pH. Then, agitation-treated and control samples (30 and 60 μM) were incubated without agitation at 37 °C. (a) Time course of fibril elongation of the agitation-treated and control samples. The elongation during the incubation was monitored by the ThT binding assay for the agitation-treated samples (●: 30 μM, ■: 60 μM) and control samples (○: 30 μM, □: 60 μM). (b) far-UV CD spectra of β2-m (30 μM) subjected to the agitation and incubation. ○: native β2-m before agitation, □: after agitation, Δ: after the agitation and incubation for 40 days. A plot of ellipticity at 220 nm of the agitation-treated β2-m against incubation time is shown in the inset. (c) EM images of the agitation-treated and control β2-m (30 and 60 μM) after the incubation. (c-1,2): agitation-treated β2-m at 30 μM (c-1) and 60 μM (c-2); (c-3,4): control β2-m at 30 μM (c-3) and 60 μM (c-4). The images of the samples at 30 μM and 60 μM were taken after incubation for 17 days and 20 days, respectively. The scale bars represent 200 nm.

in the ellipticity. These results imply that the change in secondary structure associated with the enhanced ThT fluorescence upon incubation was small enough to exclude its evaluation by CD spectroscopy.

For the two aggregated samples of 30 μM and 60 μM β2-m in Figure 4a, the presence of amyloid fibrils during the incubation was verified by EM. Namely, the EM image of the agitation-treated aggregates at 30 μM taken out after incubation for 17 days demonstrated the presence of small quantities of mature amyloid fibrils with a well-defined morphology (10−20 nm in diameter, see Figure 4c-1), although amorphous aggregates were still the most common species in the images examined. Similarly, the presence of amyloid fibrils was confirmed for the aggregated β2-m at 60 μM which was taken out after 20 days (Figure 4c-2). No fibrillar structure was observed for their control samples incubated for the same period (see Figure 4c-3 and 4c-4 for the control samples at 30 and 60 μM, respectively). Therefore, along with the increase in ThT fluorescence without the detectable lag phase, the EM images indicate elongation from an amyloid nucleus generated upon agitation-induced aggregation, although the amount of fibrils is quite small (Figure 4b).

*Amyloid Nucleation Triggered by Agitation at Neutral pH.* Then, we attempted to identify whether an amyloid nucleus is generated upon agitation-treated aggregation from β2-m in 1.0 M NaCl solution at neutral pH by (i) heat treatment to 90 °C, (ii) a jump in pH to acidic conditions, (iii) addition

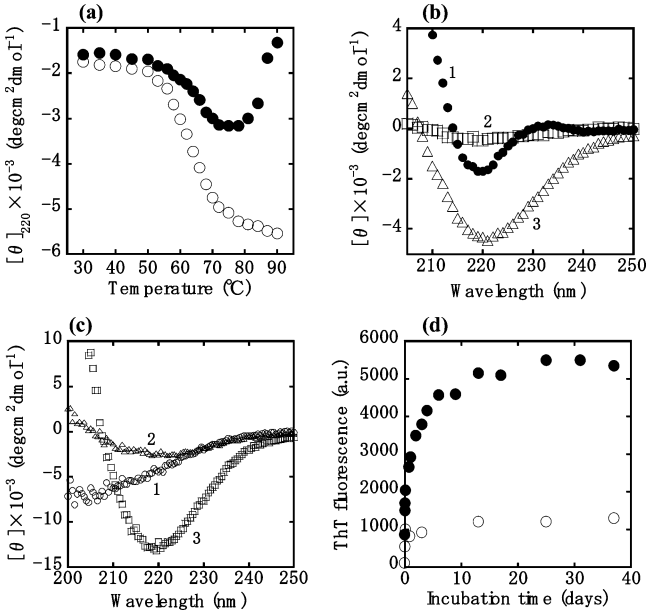


FIGURE 5: Amyloid nucleation of $\beta$2-m triggered by agitation at neutral pH. Agitation was carried out as in Figure 1 with 30 or 60 $\mu$M $\beta$2-m in 1.0 M NaCl solution at neutral pH. (a) Thermal response of the agitation-treated and agitation-free $\beta$2-m (30 $\mu$M). The samples were heated in increments of 2−2.5 °C from 30 to 90 °C in a thermoelectrically controlled cell holder attached to the polarimeter and kept for 2 min at each temperature before the ellipticity at 220 nm was recorded. (○): agitation-free sample, (●): agitation-treated sample. (b) CD spectra of the samples in panel a. The CD spectra were measured at 25 °C after cooling from 90 °C. For the aggregated sample, the measurements were twice conducted before and after homogenizing the aggregates by the sonication treatment. 1: agitation-free sample, 2: agitation-treated sample before sonication, 3: after sonication. (c) CD spectra of $\beta$2-m after the jump to an acidic pH. The agitation-treated $\beta$2-m and agitation-free $\beta$2-m (60 $\mu$M) were diluted 5 fold with 250 mM citrate buffer at pH 2.5 and milli-Q water, resulting in 12 $\mu$M $\beta$2-m, 200 mM NaCl, 50 mM citrate buffer (pH ∼2.5), and incubated without agitation for 24 h at 37 °C. The CD spectra of the samples were recorded after the incubation. For the agitation-treated sample, the measurements were twice conducted before and after homogenizing the aggregates by the sonication treatment. 1: agitation-free sample, 2: agitation-treated sample before sonication, 3: after sonication. (d) Fibril elongation of the agitation-treated $\beta$2-m in the presence of SDS. The agitation-treated $\beta$2-m and control $\beta$2-m (30 $\mu$M) were incubated at 37 °C with 0.5 mM SDS, and the fibril elongation during the incubation was monitored by the ThT binding assay. (●): agitation-treated $\beta$2-m, (○): agitation-free $\beta$2-m.

of SDS, and (iv) ultracentrifugation. First of all, to clarify the heat-induced unfolding behavior of the agitation-treated and control samples (30 $\mu$M), the changes in ellipticity at 220 nm of the samples were monitored as a function of temperature (Figure 5a). The control sample without the agitation treatment showed a typical heat-induced transition of globular proteins into a thermally unfolded state. The CD spectrum after cooling to 25 °C was the one characteristic of the native state, indicating a high reversibility (Figure 5b). In contrast, a transition-like behavior was detected for the aggregated sample, however, followed by a rapid rise of the ellipticity in the temperature range above 80 °C (Figure 5a). Although the CD spectrum after cooling exhibited an unusual pattern featured by aggregated protein molecules, it became a clearer $\beta$-sheet pattern with a minimum at 220 nm after the sonication treatment that induces the dispersion of aggregates (Figure 5b). Thus, the transition-like curve obtained for the aggregated sample implies that the negative increase in CD intensity during the heating process arises from the conformational change into the unfolded state and the attendant conversion into the $\beta$-sheet structure, in which the thermally unfolded protein molecules are incorporated into the existing amyloid nucleus. At high temperature above 80 °C, the aggregation of fibrils causes a decrease in intensity, resulting in the unusual CD spectrum.

Second, the aggregated and control samples of 60 $\mu$M $\beta$2-m in 1.0 M NaCl solution were diluted 5 fold with 250 mM citrate buffer at pH 2.5 and Milli-Q water, resulting in 12 $\mu$M $\beta$2-m, 200 mM NaCl, and 50 mM citrate buffer. The two diluted samples were subjected to incubation without agitation at 37 °C for 24 h. The CD measurements were performed at 25 °C for these samples after the incubation, revealing a distinct difference in their spectra (Figure 5c); the control sample had a spectrum typical of acid-unfolded $\beta$2-m while the aggregated sample exhibited an unusual spectrum that has been seen for aggregated fibrils. Importantly, when the aggregated sample was dispersed by the sonication treatment, the spectrum turned to one typical of a $\beta$-sheet structure with a minimum at 220 nm, indicating that the amyloid nucleus existing in the aggregated sample was extended with the acid unfolded molecules.

Third, the agitation-treated aggregates of 30 $\mu$M $\beta$2-m in 1.0 M NaCl solution were incubated without agitation at 37 °C in the presence of 0.5 mM SDS with the aim of accelerating the conversion into amyloid fibrils. SDS, an anionic detergent, has been reported to have the effect of destabilizing the compact native conformation of $\beta$2-m as well as stabilizing the amyloid fibrils generated at neutral pH, resulting in an acceleration of the fibrillation of $\beta$2-m in the presence of preformed seed fibrils (*23*, *35*). The effect was dependent on the concentration of SDS and maximal at approximately 0.5 mM, around the critical micelle concentration of SDS (*23*). Thus, a promotive effect of SDS on the fibrillation by the agitation−incubation method was expected at neutral pH. Consistent with such expectations, a much larger increase in ThT fluorescence was observed without a detectable lag phase in the presence of 0.5 mM SDS, and the increase reached a plateau after 20 days of incubation, indicating the formation of amyloid fibrils with a significant amount of organized $\beta$-structure on this time scale (Figure 5d). The fibrillation of the aggregated sample in the presence of SDS was confirmed by EM (data not shown). The addition of SDS to the $\beta$2-m solution without the agitation treatment under the same conditions caused a slight increase in ThT fluorescence and a rapid saturation (Figure 5d), suggesting the SDS-induced association of the protein molecules as indicated by a previous study (*35*). The time-dependent kinetics showing no detectable lag phase in the fibril elongation reaction provides additional evidence for amyloid nucleation upon agitation.

Finally, to estimate the amount of aggregate formed by agitation, sedimentation velocity experiments were conducted for two samples at neutral pH: agitation-free $\beta$2-m at 48 $\mu$M in 1.0 M NaCl solution (i.e., control sample) and the same sample subjected to the agitation treatment. The spinning was conducted at 181000*g* after a preliminary spinning at 27000*g*. The movements of the boundary of both samples during the spinning at 181000*g* were recorded, clearly showing the broadening of the boundary with diffusion (Figure 6a and 6b). For the two samples, the

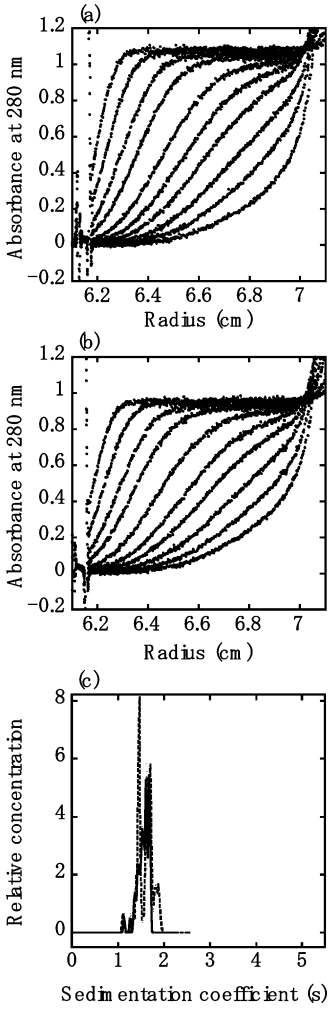


FIGURE 6: Ultracentrifugation-based analysis of the agitation-treated and agitation-free $\beta$2-m at 37 °C. Agitation was conducted as in Figure 1 with 48 $\mu$M $\beta$2-m in the presence of 1.0 M NaCl at neutral pH. (a and b) Sedimentation profiles of agitation-free $\beta$2-m (a) and agitation-treated $\beta$2-m (b) at neutral pH. For two samples, each sedimentation pattern was recorded by monitoring the absorbance at 280 nm, in which several traces at the same time intervals were presented. (c) The distribution of sedimentation coefficients ($S_{20,w}$) obtained from the sedimentation velocity data. Continuous line: agitation-treated $\beta$2-m dotted line: agitation-free $\beta$2-m.

sedimentation coefficients were estimated using the sedimentation velocity data, showing no remarkable difference for the association of the protein molecules (Figure 6c); the main component corresponding to the sedimentation coefficient of 1.5 is monomeric $\beta$2-m. Importantly, the concentration at the plateau of the initial boundary movements (i.e., maximum absorbance at 280 nm) for the agitation-treated sample was lower approximately by 9% than that for the control sample. This decrease in absorbance could be attributed to the rapid sedimentation of the aggregates formed upon agitation during the preliminary spinning at 27000*g*. Although we attempted to evaluate the sedimentation coefficient for the aggregated component, we were unsuccessful because of the rapid sedimentation even at 3000 rpm, confirming that the aggregates formed upon agitation include a polymerized species (i.e., amyloid nucleus). Taking the results together, the agitation-treated sample mainly consists of two components, monomers in the native state (sedimentation coefficient ~1.5) and enormous aggregates. In the process of agitation forming the aggregates, amyloid nucleation is presumed to be triggered via transiently generated oligomers at neutral pH where the native structure is highly stable. The amount of amyloid nucleus was estimated to be at most 9% of all the protein molecules under the present conditions, which might not significantly contribute to the change in CD intensity as shown in Figure 4b.

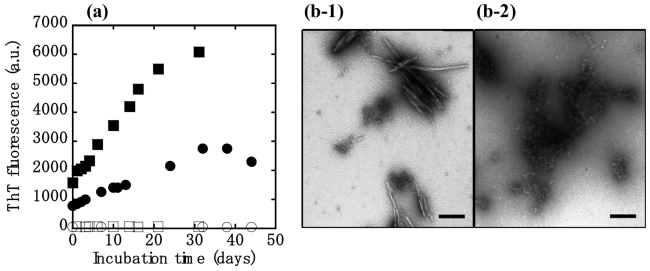


FIGURE 7: Conversion of HEWL in the native state into mature amyloid fibrils at neutral pH. Agitation was conducted as in Figure 1 with 30 and 60 $\mu$M HEWL in the presence of 0.5 M NaCl at neutral pH. Agitation-treated and control samples were incubated without agitation at 37 °C. (a) Time course of fibril elongation of the agitation-treated HEWL (30 and 60 $\mu$M). The fibril growth of the agitation-treated samples was monitored at various points in time by the ThT binding assay. ●: 30 $\mu$M, ■: 60 $\mu$M. The binding of ThT to the control samples without the agitation treatment was similarly examined. ○: 30 $\mu$M, □: 60 $\mu$M. (b) EM images of the agitation-treated and control samples. (b-1) agitation-treated HEWL (30 $\mu$M); (b-2) agitation-free HEWL (30 $\mu$M). The images were taken after incubation for 30 days. The scale bars represents 200 nm.

*Conversion of HEWL in the Native State into Amyloid Fibrils at Neutral pH.* Amyloid nucleation by agitation was also achieved with a different protein, HEWL, at neutral pH, which is one of the earliest characterized and most studied globular proteins (*36*). Its 129 amino acid residues, that are cross-linked by four disulfide bonds, fold into two domains ($\alpha$ and $\beta$) (*37*). Detailed studies about the fibrillation of HEWL as a model protein have shown that prolonged incubation under the conditions of acidic pH (pH 1.6−2) and elevated temperature (57−70 °C) initiate the fibrillation of this protein (*31*, *38*−*40*). As in the case of $\beta$2-m in Figure 4a, two HEWL solutions at 30 and 60 $\mu$M were agitated in 0.5 M NaCl solutions, and incubated without agitation at 37 °C, in which the pH of the buffer-free solvent was 7.0−7.6. The agitation induced the formation of aggregates as indicated by the increase in light scattering (see Figure 1 for 30 $\mu$M HEWL). The incubation of the aggregated samples resulted in an increase of fluorescence in the ThT binding assay without a lag phase, suggesting the growth of amyloid fibrils, compared with those obtained with the control samples (Figure 7a).

The morphology after the prolonged incubation for 30 days was characterized based on the EM; the agitation-treated aggregates definitely revealed the presence of amyloid fibrils with a well-defined morphology (see Figure 7b-1 for the sample at 30 $\mu$M), whereas the control samples subjected to the same incubation exhibited an abundance of amorphous-like aggregates (Figure 7b-2). Together with the results of the ThT binding assay, these findings strongly suggest that amyloid nucleation was triggered during the agitation-treated aggregation, followed by the elongation of fibrils upon incubation without agitation at 37 °C.

## DISCUSSION

*Effect of Aggregates or Oligomers on Fibrillation.* There have been several reports that amyloid fibrils are spontaneously formed via the accumulation of oligomers or spherical aggregates without seed fibrils (*41*−*47*). For example, the formation of spherical aggregates by agitation of $\beta$2-m preceded spontaneous fibrillation under acidic conditions, consistent with the results obtained at pH 2.5 in this study (*41*). Very recently, under acidic conditions, the transient nature of early oligomeric species associated with the formation of amyloid fibrils of $\beta$2-m was monitored by electrospray ionization mass spectrometry, showing that monomers, dimers, trimers, and tetramers are involved in the nucleation that leads to the elongation into mature amyloid fibrils (*48*). Copper ion has been indicated to mediate the oligomerization of native-like precursors of $\beta$2-m, which precedes the amyloid formation at pH 7.4 (*24*, *49*). At least, in the case of $\beta$2-m, the formation of spherical aggregates or oligomers seems to be followed by fibril extension, in which well-defined amyloid fibrils develop from these initial aggregates or oligomers, although the mechanism of fibrillation assisted by aggregates or oligomers remains unknown. Generally, the formation of oligomers or spherical aggregates is a complex process due to the inherent heterogeneity and transient nature early on when oligomers and monomers are in equilibrium and is strongly influenced by a variety of factors such as temperature, protein concentration, and ionic strength and pH of the solution (*42*). Therefore, more systematic studies are needed to clarify the role of oligomers or initial aggregates in the formation of amyloid fibrils, particularly under physiological neutral pH conditions without detergents, denaturants, or organic solvents that cause a destabilization of protein molecules.

*Amyloid Nucleation Triggered by Agitation.* Agitation-induced aggregation of $\beta$2-m is promoted in the presence of NaCl, as indicated by the enhanced light scattering intensity (Figure 1), consistent with previous results (*28*). Importantly, in this study, it was found that the amyloid nucleus of $\beta$2-m is produced during agitation-induced aggregation in the presence of NaCl which will screen the charges present on the protein and promote protein association along with the effect of accelerating diffusion of soluble monomers by stirring. During moderate aggregation, the probability of generating an amyloid nucleus would be enhanced via specific interactions between adjacent molecules. The efficiency with which the amyloid nucleus was generated and the subsequent elongation occurred was significantly enhanced at pH 2.5 where the protein is acid unfolded, as shown by the changes in the CD spectrum upon agitation and during the incubation (Figure 2c). This could be accounted for by the conformational flexibility allowing the structural rearrangement required to form a fibril nucleus (*50*). In the present study, the aggregation of the protein solutions was performed in the cell of an ITC by stirring the attached cylinder for 24 h at 310 nm and 37 °C, standard conditions to induce the aggregation of $\beta$2-m which were selected based on a previous study (*28*). The agitation was found to trigger the fibril nucleation of two proteins, $\beta$2-m and HEWL, under entirely native conditions.

A nucleation−polymerization model has been proposed to explain the general mechanism of by which amyloid fibrils form in vitro (*14*, *51*). The model consists of two processes: nucleation and polymerization. The nucleation process, in which a number of monomeric precursor molecules associate, producing a minimal fibril unit, represents the rate-determining step in the formation of amyloid fibrils. Once the nucleus is formed, however, subsequent growth proceeds rapidly via the incorporation of the monomers into the ends of nucleated fibrils. A variety of experiments have demonstrated that the fibrillation of amyloidogenic proteins including $\beta$2-m involves a well-defined lag phase, that corresponds to the nucleation process, before the formation of mature, well-defined amyloid fibrils (*6*, *14*, *51*−*54*). In this context, the agitation caused by stirring the protein solution in the presence of salt leads to aggregation during which amyloid nucleation is triggered, resulting in elongation without a lag phase upon incubation without agitation (Figure 8). As shown in Figure 2a−c, in the seed-dependent extension reaction at pH 2.5 and 37 °C, fibrils are extended via the consecutive association of unfolded $\beta$2-m onto the ends of the fibrils (*14*, *54*, *55*). Kardos et al. have shown that most of the acid-unfolded $\beta$2-m (>99%) are converted into the fibrils at pH 2.5 (*54*).

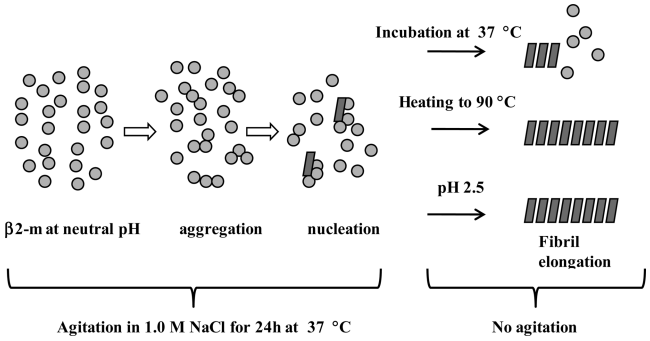


FIGURE 8: A proposed scheme of amyloid nucleation of $\beta$2-m under neutral pH conditions including 1.0 M NaCl. During the process of agitation for 24 h at 37 °C at neutral pH where the native conformation is highly stable, amyloid nucleation is triggered via transiently accumulated oligomeric species by agitation. The probability of inducing fibril nucleation is enhanced via agitation-treated aggregation in the presence of salt. The fibril nucleus formed in the aggregates is extended upon incubation without agitation at 37 °C, by the heat treatment, and the jump in pH to 2.5.

As described in the Introduction, $\beta$2-m can form at least two kinds of fibrils with different morphologies at pH 2.5: salt-induced WL fibrils and mature amyloid fibrils. The amyloid fibrils formed from the acid-unfolded state by the agitation−incubation method at pH 2.5 showed a well-organized morphology corresponding to the latter. Interestingly, the aggregated WL fibrils after incubation for several days appeared to be a mixture of WL fibrils and mature amyloid fibrils (Figure 3c-2), indicating that even the WL fibrils, considered to be a dead-end product, can produce a nucleus of mature fibrils upon agitation. Previously (*29*), when WL fibrils aggregated by agitation were heated by a DSC instrument, their conversion into mature amyloid fibrils was achieved, accompanied by a sigmoidal decrease in heat capacity of the protein solution, implying that there is a distinct energy barrier between the two fibrillar structures. Together with this result (*29*), the present findings indicate that the mature amyloid fibrils are thermodynamically more stable than the WL fibrils.

Under the conditions at neutral pH and 37 °C, partially folded β2-m and HEWL are rare, but would be populated to a certain extent at equilibrium. In fact, a study using capillary electrophoresis showed that a partially folded β2-m exists in equilibrium with the native β2-m under physiological conditions (*20*). A partially folded, equilibrium molten globule state of HEWL has been shown to be present at lower pH (∼1.0) where the native structure is destabilized (*56*), suggesting that such a species would potentially be populated in surroundings at neutral pH and higher temperature (i.e., 37 °C). Thus, the equilibrium population of a partially folded form might explain the slow elongation of the amyloid nucleus for β2-m and HEWL at neutral pH and 37 °C (Figure 4a and 7a).

Recently, cross-β spine, three-dimensional domain swapping, and their combined models have been reported to explain amyloid fibril formation (*57*). These models propose that structural rearrangement in a limited region of the native structure induces an assembly-competent surface that forms cross-β structure. The possibility that a native-like protein can participate in aggregation has been suggested in the formation of amyloid fibrils by some proteins such as acylphophatase (*58*), ribonuclease A (*59*), and cystatin (*60*). Although we cannot recognize the marked difference in morphology between the β2-m fibrils formed under the acidic and neutral pH conditions (Figure 2d-2 and Figure 4c-1,2), the mechanisms of fibril formation under these conditions may be possibly quite distinct. A noteworthy point in Figure 6 is that the main component other than the agitation-induced aggregates including the amyloid nucleus is monomeric β2-m. That is to say, no oligomers that formed between the monomer and fibril nucleus were detected in the sedimentation velocity analysis at neutral pH where the native conformation is highly stable, suggesting that the agitation-induced aggregates are formed via transient oligomer species and become thermodynamically stable after amyloid nucleation is triggered in the aggregation process (Figure 8).

*Aggregation of Generated Fibrils.* The ThT fluorescence of the agitation-treated aggregates of acid-unfolded β2-m in the absence of NaCl at pH 2.5 increased significantly without a lag time, reaching a high value upon incubation (Figure 2a). However, in the cases of the WL fibrillar and native forms in the presence of NaCl, the fluorescence value decreased after the initial increase (Figures 3a and 4a), suggestive of the propensity of extended fibrils to aggregate under the experimental conditions including NaCl. We consider that the decrease in the enhanced ThT signal is partly explained by the difference in net charge on the fibrils. The isoelectric point of β2-m is around 6, and the net charge at pH 2.5 and 7.0 is +17 and −3, respectively, implying that the charge repulsion is large at pH 2.5 and small at neutral pH. The extended fibrils at neutral pH could cluster due to the decreased net charge. Furthermore, as the charge present on the protein will be screened at high NaCl concentrations at pH 2.5, the gathering of mature fibrils converted from the WL fibrils could be promoted in the presence of 0.5 M NaCl, causing the decrease of ThT-binding sites. In the presence of SDS that may penetrate into the inside of the aggregated proteins, the destabilization or partial unfolding of β2-m might occur, providing more assembly-competent molecules (*23*). Furthermore, the binding of SDS onto growing fibrils might provide for additional stabilization of the fibrils (*23*), resulting in the rapid increase and the subsequent saturation of ThT fluorescence during the incubation period (Figure 5d).

## CONCLUSIONS

The effects of physiologically relevant factors upon the fibrillation of β2-m have been proposed to explain the molecular mechanism behind DRA. These include components commonly found in amyloid deposits of β2-m: glycosaminoglycans (*22*, *34*, *61*), proteoglycans (*34*, *61*), collagen (*34*, *62*), apolipoprotein E (*34*, *63*), etc. It has been reported that amyloid seeds are stabilized in the presence of some of these components, providing interaction sites into which assembly-competent molecules can be effectively incorporated (*34*). Furthermore, the fibril formation is driven by further binding of the components to the growing fibrils. Despite the increasing knowledge of β2-m amyloid fibril formation in vitro, a key question remains unsolved: how is amyloid nucleation triggered? Generally, it is accepted that one of the most critical factors of DRA is the 60-fold increased level of β2-m (i.e., >5 μM) (*4*−*6*). However, it takes on average of >10 years to form substantial amyloid deposits. Akin to the behavior of other amyloidogenic proteins, transient unfolding of the protein is required to initiate fibrillation, presumably through the exposure of new assembly-competent sites (*50*). In this study without the physiologically relevant factors described above, for β2-m and HEWL, amyloid nucleation at neutral pH was triggered in the process of the agitation-treated aggregation in the presence of NaCl which could cause local or transient unfolding or distortion. It is therefore plausible that oligomerization or aggregation represents an essential step leading to the fibril nucleation. Our experimental findings lead us to believe that fibrillation is indeed an intrinsic property of proteins, as suggested by Dobson (*64*); although various compounds have an influence in modulating the processes of fibrillation of β2-m in vivo, as observed in the presence of SDS in this study, the precursor proteins could form fibrils by themselves under physiological conditions. The present study suggests the importance of the effect of aggregation on the onset of the fibrillation of β2-m, in which amyloid nucleation is triggered upon aggregation that would be promoted as the protein concentration increases.

## ACKNOWLEDGMENT

Electron micrographs were taken at the Research Center for Ultrahigh Voltage Electron Microscopy, Osaka University, Japan.

## REFERENCES

1. Bjorkman, P. J., Saper, M. A., Samraoui, B., Bennett, W. S., Strominger, J. L., and Wiley, D. C. (1987) Structure of the human class I histocompatibility antigen, HLA-A2, *Nature 329*, 506−512.
2. Verdone, G., Corazza, A., **V**iglino, P., Pettirossi F., Giorgetti, S., Mangione, P., Andreola A., Stoppini, M., Bellotti, V., and Esposito, G. (2002) The solution structure of human β2-microglobulin reveals the prodromes of its amyloid transition, *Protein Sci. 11*, 487−499.
3. Trinh, C. H., Smith, D. P., Kalverda, A. P., Phillips, S. E. V., and Radford, S. E. (2002) Crystal structure of monomeric human β-2-microglobulin reveals clues to its amyloidogenic properties, *Proc. Natl. Acad. Sci. U.S.A. 99*, 9771−9776.

4. Floege, J., and Ketteler, M. (2001) $\beta_2$-Microglobulin-derived amyloidosis: an update, *Kidney Int. 78*, S164−S171.
5. Yamamoto, S., and Gejyo, F. (2005) Historical background and clinical treatment of dialysis-related amyloidosis, *Biochim. Biophys. Acta 1753*, 4−10.
6. Radford, S. E., Gosal, W. S., and Platt, G. W. (2005) Towards an understanding of the structural molecular mechanism of $\beta_2$-microglobulin amyloid formation in vitro, *Biochim. Biophys. Acta 1753*, 51−63.
7. Selkoe, D. J. (2003) Folding proteins in fatal ways, *Nature 426*, 900−904.
8. Chiti, F., and Dobson, C. M. (2006) Protein misfolding, functional amyloid, and human disease, *Annu. Rev. Biochem. 75*, 333−366.
9. Makin, O. S., and Serpell, L. C. (2005) Structures for amyloid fibrils, *FEBS. J. 272*, 5950−5961.
10. Chanard, J., Bindi, P., Lavaud, S., Toupance, O., Maheut, H., and Lacour, F. (1989) Carpal tunnel syndrome and type of dialysis membrane, *Br. Med. J. 298*, 867−868.
11. van Ypersele de Strihou, C., Jadoul, M., Malghem, J., Maldague, B., and Jamart, J. (1991) Effect of dialysis membrane and patient's age on signs of dialysis-related amyloidosis. The working party on dialysis amyloidosis, *Kidney Int. 39*, 1012−1019.
12. Hong, D.-P., Gozu, M., Hasegawa, K., Naiki, H., and Goto, Y. (2002) Conformation of $\beta_2$-microglobulin amyloid fibrils analyzed by reduction of the disulfide bond, *J. Biol. Chem. 277*, 21554−21560.
13. Gosal, W. S., Morten, I. J., Hewitt, E. W., Smith, D. A., Thomson, N. H., and Radford, S. E. (2005) Competing pathways determine fibril morphology in the self-assembly of $\beta_2$-microglobulin into amyloid, *J. Mol. Biol. 351*, 850−864.
14. Naiki, H., Hashimoto, N., Suzuki, S., Kimura, H., Nakakuki, K., and Gejyo, F. (1997) Establishment of a kinetic model of dialysis-related amyloid fibril extension in vitro, *Amyloid 4*, 223−232.
15. Ross, C. A., and Poirier, M. A. (2004) Protein aggregation and neurodegenerative disease, *Nature Med. 10*, S10−S17.
16. Modler, A. J., Gast, K., Lutsch, G., and Damaschun, G. (2003) Assembly of amyloid protofibrils *via* critical oligomers-A novel pathway of amyloid formation, *J. Mol. Biol. 325*, 135−148.
17. Hurshman, A. R., White, J. T., Powers, E. T., and Kelly, J. W. (2004) Transthyretin aggregation under partially denaturing conditions is a downhill polymerization, *Biochemistry 43*, 7365−7381.
18. Carrotta, R., Manno, M., Bulone, D., Martorana, V., and San, Biagio, P. L. (2005) Protofibril formation of amyloid $\beta$-protein at low pH via a non-cooperative elongation mechanism, *J. Biol. Chem. 280*, 30001−30008.
19. Bader, R., Bamford, R., Zurdo, J., Luisi, B. F., and Dobson, C. M. (2006) Probing the mechanism of amyloidogenesis through a tandem repeat of the PI3-SH3 domain suggests a generic model for protein aggregation and fibril formation, (2006) *J. Mol. Biol. 356*, 189−208.
20. Chiti, F., De Lorenzi, E., Grossi, S., Mangione, P., Giorgetti, S., Caccialanza, G., Dobson, C. M., Merlini, G., Ramponi, G., and Bellotti, V. (2001) A partially structured species of $\beta_2$-microglobulin is significantly populated under physiological conditions and involved in fibrillogenesis, *J. Biol. Chem. 276*, 46714−46721.
21. Jahn, T. R., Parker, M. J., Homans, S. W., and Radford, S. E. (2006) Amyloid formation under physiological conditions proceeds via a native-like folding intermediate, *Nat. Struct. Mol. Biol. 13*, 195−201.
22. Yamamoto, S., Yamaguchi, I., Hasegawa, K., Tsutsumi, S., Goto, Y., Gejyo, F., and Naiki, H. (2004) Glycosaminoglycans enhance the trifluoroethanol-induced extension of $\beta_2$-microglobulin-related amyloid fibrils at a neutral pH, *J. Am. Soc. Nephrol. 15*, 126−133.
23. Yamamoto, S., Hasegawa, K., Yamaguchi, I., Tsutsumi, S., Kardos, J., Goto, Y., Gejyo, F., and Naiki, H. (2004) Low concentrations of sodium dodecyl sulfate induce the extension of $\beta_2$-microglobulin-related amyloid fibrils at a neutral pH, *Biochemistry 43*, 11075−11082.
24. Morgan, C. J., Gelfand, M., Atreya, C., and Miranker, A. D. (2001) Kidney dialysis-associated amyloidosis: a molecular role for copper in fiber formation, *J. Mol. Biol. 309*, 339−345.
25. Ohhashi, Y., Kihara, M., Naiki, H., and Goto, Y. (2005) Ultrasonication-induced amyloid formation of $\beta_2$-microglobulin, *J. Biol. Chem. 280*, 32843−32848.
26. Esposito, R., Michelutti, R., Verdone, G., Viglino, P., Hernández, H., Robinson, C. V., Amoresano, A., Dal, Piaz, F., Monti, M., Pucci, P., Mangione, P., Stoppini, M., Merlini, G., Ferri, G., and Bellotti, V. (2000) Removal of the N-terminal hexapeptide from human $\beta_2$-microglobulin facilitates protein aggregation and fibril formation, *Protein Sci. 9*, 831−845.
27. Jones, S., Smith, D. P., and Radford, S. E. (2003) Role of the N and C-terminal strands of beta 2-microglobulin in amyloid formation at neutral pH, *J. Mol. Biol. 330*, 935−941.
28. Sasahara, K., Yagi, H., Naiki, H., and Goto, Y. (2007) Heat-induced conversion of $\beta_2$-microglobulin and hen egg-white lysozyme into amyloid fibrils, *J. Mol. Biol. 372*, 981−991.
29. Sasahara, K., Yagi, H., Naiki, H., and Goto, Y. (2007) Heat-triggered conversion of protofibrils into mature amyloid fibrils of $\beta_2$-microglobulin, *Biochemistry 46*, 3286−3293.
30. Chiba, T., Hagihara, Y., Higurashi, T., Hasegawa, K., Naiki, H., and Goto, Y. (2003) Amyloid fibril formation in the context of full-length protein. Effects of proline mutations on the amyloid fibril formation of $\beta_2$-microglobulin, *J. Biol. Chem. 278*, 47016−47024.
31. Arnaudov, L. N., and de Vries, R. (2005) Thermally induced fibrillar aggregation of hen egg white lysozyme, *Biophys. J. 88*, 515−526.
32. LeVine, H. (1999) Quantification of $\beta$-sheet amyloid fibril structures with thioflavin-T. *Methods Enzymol, 309*, 274−284.
33. Sasahara, K., Naiki, H., and Goto, Y. (2005) Kinetically controlled thermal response of $\beta_2$-microglobulin amyloid fibrils, *J. Mol. Biol. 352*, 700−711.
34. Myers, S. L., Jones, S., Jahn, T. R., Morten, I. J., Tennent, G. A., Hewitt, E. W., and Radford, S. E. (2006) A systematic study of the effect of physiological factors on $\beta_2$-microglobulin amyloid formation at neutral pH, *Biochemistry 45*, 2311−2321.
35. Kihara, M., Chatani, E., Sakai, M., Hasegawa, K., Naiki, H., and Goto, Y. (2005) Seeding-dependent maturation of $\beta_2$-microglobulin amyloid fibrils at neutral pH, *J. Biol. Chem. 280*, 12012−12018.
36. Dobson. C. M., Evans, P. A., and Radford, S. E. (1994) Understanding how proteins fold: the lysozyme story so far, *Trends Biochem. Sci. 19*, 31−37.
37. Blake, C. C. F., Koenig, D. F., Mair, G. A., North, A. C. T., Phillips, D. C., and Sarma, V. R. (1965) Structure of hen egg-white lysozyme. A three-dimensional fourier synthesis at 2Å resolution, *Nature 206*, 757−761.
38. Krebs, M. R. H., Wilkins, D. K., Chung, E. W., Pitkeathly, M. C., Chamberlain, A. K., Zurdo, J., Robinson, C. V., and Dobson, C. M. (2000) Formation and seeding of amyloid fibrils from wild-type hen lysozyme and a peptide fragment from the $\beta$-domain, *J. Mol. Biol. 300*, 541−549.
39. Frare, E., Polverino de Laureto, P., Zurdo, J., Dobson, C. M., and Fontana, A. (2004) A highly amyloidogenic region of hen lysozyme, *J. Mol. Biol. 340*, 1153−1165.
40. Mishra, R., Sörgjerd, K., Nyström, S., Nordigården, A., Yu, Y-C., and Hammarström, P. (2007) Lysozyme amyloidogenesis is accelerated by specific nicking and fragmentation but decelerated by intact protein binding and conversion, *J. Mol. Biol. 366*, 1029−1044.
41. Kad, N. M., Myers, S. L., Smith, D. P., Smith, D. A., Radford, S. E., and Thomson, N. H. (2003) Hierarchical assembly of $\beta_2$-microglobulin amyloid *in vitro* revealed by atomic force microscopy, *J. Mol. Biol. 330*, 785−797.
42. Zurdo, J., Guijarro, J. I., Jiménez, J. L., Saibil, H. R., and Dobson, C. M. (2001) Dependence on solution conditions of aggregation and amyloid formation by an SH3 domain, *J. Mol. Biol. 311*, 325−340.
43. Lashuel, H. A., Petre, B. M., Wall, J., Simon, M., Nowak, R. J., Walz, T., and Lansbury, P. T. (2002) α-Synuclein, especially the Parkinson's disease-associated mutants, forms pore-like annular and tubular protofibrils, *J. Mol. Biol. 322*, 1089−1102.
44. Nettleton, E. J., Tito, P., Sunde, M., Bouchard, M., Dobson, C. M., and Robinson, C. V. (2000) Characterization of the oligomeric states of insulin in self-assembly and amyloid fibril formation by mass spectrometry, *Biophys. J. 79*, 1053−1065.
45. Poirier, M. A., Li, H., Macosko, J., Cai, S., Amzel, M., and Ross, C. A. (2002) Huntingtin spheroids and protofibrils as precursors in polyglutamine fibrillation, *J. Biol. Chem. 277*, 41032−41037.
46. Bucciantini, M., Giannoni, E., Chiti, F., Baroni, F., Formigli, L., Zurdo, J., Taddei, N., Ramponi, G., Dobson, C. M., and Stefani, M. (2002) Inherent toxicity of aggregates implies a common mechanism for protein misfolding diseases, *Nature 416*, 507−511.
47. Qin, Z., Hu, D., Zhu, M., and Fink, A. L. (2007) Structural characterization of the partially folded intermediates of an

immunoglobulin light chain leading to amyloid fibrilllation and amorphous aggregation, *Biochemistry 46*, 3521−3531.
48. Smith, A. M., Jahn, T. R., Ashcroft, A. E., and Radford, S. E. (2006) Direct observation of oligomeric species formed in the early stages of amyloid fibril formation using electrospray ionization mass spectrometry, *J. Mol. Biol. 364*, 9−19.
49. Calabrese, M. F., and Miranker, A. D. (2007) Formation of a stable oligomer of $\beta$-2 microglobulin requires only transient encounter with Cu(II), *J. Mol. Biol. 367*, 1−7.
50. Uversky, V. N., and Fink, A. L. (2004) Conformational constraints for amyloid fibrillation: the importance of being unfolded, *Biochim. Biophys. Acta 1698*, 131−153.
51. Jarrett, J. T., and Lansbury, P. T., Jr. (1993) Seeding "one-dimensional crystallization" of amyloid: A pathogenic mechanism in Alzheimer's disease and scrapie? *Cell 73*, 1055−1058.
52. Lomakin, A., Chung, D. S., Benedek, G. B., Kirschner, D. A., and Teplow, D. B (1996) On the nucleation and growth of amyloid beta-protein fibrils: detection of nuclei and quantitation of rate constants, *Proc. Natl. Acad. Sci. U.S.A. 93*, 1125−1129.
53. Serio, T. R., Cashikar, A. G., Kowal, A. S., Sawicki, G. J., Moslehi, J. J., Serpell, L., Arnsdorf, M. F., and Lindquist, S. L. (2000) Nucleated conformational conversion and the replication of conformational information by a prion determinant, *Science 289*, 1317−1321.
54. Kardos, J., Yamamoto, K., Hasegawa, K., Naiki, H., and Goto, Y. (2004) Direct measurement of the thermodynamic parameters of amyloid formation by isothermal titration calorimetry, *J. Biol. Chem. 279*, 55308−55314.
55. Sasahara, K., Naiki, H., and Goto, Y. (2006) Exothermic effects observed upon heating of $\beta_2$-microglobulin monomers in the presence of amyloid seeds, *Biochemistry 45*, 8760−8769.
56. Sasahara, K., Demura, M., and Nitta, K. (2000) Partially unfolded equilibrium state of hen lysozyme studied by circular dichroism spectroscopy, *Biochemistry 39*, 6475−6482.
57. Nelson, R., and Eisenberg, D. (2006) Structural models of amyloid-like fibrils, *Adv. Protein Chem. 73*, 235−282.
58. Plakoutsi, G., Taddei, N, Stefani, M., and Chiti, F. (2004) Aggregation of the acylphosphatase from *sulfolobus solfataricus*. The folded and partially unfolded states can both be precursors for amyloid formation, *J. Biol. Chem. 279*, 14111−14119.
59. Sambashivan, S., Liu, Y., Sawaya, M. R., Gingery, M., and Eisenberg, D. (2005) Amyloid-like fibrils of ribonuclease A with three-dimensional domain-swapped and native-like structure, *Nature 437*, 266−269.
60. Sanders, A., Jeremy Craven, C., Higgins, L. D., Giannini, S., Conroy, M. J., Hounslow, A. M., Waltho, J. P., and Staniforth, R. A. (2004) Cystatin forms a tetramer through structural rearrangement of domain-swapped dimmers prior to amyloidogenesis, *J. Mol. Biol. 336*, 165−178.
61. Yamaguchi, I., Suda, H., Tsuzuike, N., Seto, K., Seki, K., Yamaguchi, Y., Hasegawa, K., Takahashi, N., Yamamoto, S., Gejyo, F., and Naiki, H. (2003) Glycosaminoglycan and proteoglycan inhibit the depolymerization of $\beta$2-microglobulin amyloid fibrils in vitro, *Kidney Int. 64*, 1080−1088.
62. Relini, A., Canale, C., De, Stefano, S., Rolandi, R., Giorgetti, S., Stoppini, M., Rossi, A., Fogolari, F., Corazza, A., Esposito, G., and Gliozzi, A. (2006) Collagen plays an active role in the aggregation of $\beta_2$-microglobulin under physiopathological conditions of dialysis-related amyloidosis, *J. Biol. Chem. 281*, 16521−16529.
63. Yamaguchi, I., Hasegawa, K., Takahashi, N., Gejyo, F., and Naiki, H. (2001) Apolipoprotein E inhibits the depolymerization of $\beta$2-microglobulin-related amyloid fibrils at a neutral pH, *Biochemistry 40*, 8499−8507.
64. Dobson, C. M. (2003) Protein folding and misfolding, *Nature 426*, 884−890.

BI701968G